typeset using JPSJ.sty <ver.0.8>

Renormalized Perturbation Approach for Examination of Itinerant-Localized Duality Model for Strongly Correlated Electron Systems

Yukihiro OKUNO*, Osamu NARIKIYO[1] and Kazumasa MIYAKE[1]

Department of Physics, Faculty of Science, Kyoto University, Kyoto 606

[1]*Department of Material Physics, Faculty of Engineering Science, Osaka University, Toyonaka 560*

(Received March 11, 1997)

We present a microscopic examination for the itinerant-localized duality model which has been proposed to understand anomalous properties of strongly correlated systems like the heavy fermions by Kuramoto and Miyake, and also useful to describe the anomalous properties of the high-T_c cupurates. The action of the duality model consists of two components of dynamical degrees of freedom. One of them is coherent itinerant degree of fermion and the other is incoherent localized one describing mainly the spin which has not been explicitly considered so far. We show that the thermodynamic potential of the strongly interacting Hubbard model can be rearranged in the form of duality model on the basis of renormalized perturbation expansion of the Luttinger-Ward functional if the one-particle spectral weight exhibits triple peak structure. We also examine the incoherent degrees of freedom described as a "localized spin" and show on the basis of the pertubation expansion that there exists commensurate superexchange-type interaction among the "localized spins".

KEYWORDS: itinerant-localized duality model, strongly correlated systems, superexchange interaction

§1. Introduction

The Fermi liquid theory offers us a very powerful tool for describing the low energy properties of strongly correlated fermions. While it was first devised by Landau[1)] to analyse the physics of liquid ^{3}He, its general and profound value has been recognized through the application to the many areas of correlated fermion systems such as Kondo problem for instance.[2,3)] But it is also true that there are many phenomena which at a first glance cannot be explained by applying the Fermi liquid theory in its simple form. For example, heavy fermions and the high T_c cuprates offer such phenomena. In the former they are the metamagnetic behavior and the extremely weak antiferromagnetism in the metallic phase. In the latter case they are "spin-gap" behavior and "spin-charge separation aspect", and the controversy about the applicability and limitation of the

* e-mail: okuno@aquarius.mp.es.osaka-u.ac.jp

Fermi liquid theory have been arisen. Itinerant-localized duality model, which has been proposed as a quantum phenomenology by Kuramoto and Miyake,[4] looks for the origin of such phenomena with the intermediate energy scale in an explicit treatment of the incoherent contribution which is renormalized in quasiparticle in the ordinary Fermi liquid theory. It has been applied not only to the heavy fermions systems,[5,6] but also the understanding the anomalous properties of high-T_c cuprates.[7,8,9]

This model is based on the physical picture that, through the renormalization group evolution to the fixed point of such strong correlated electron systems, there is an intermediate stage where both the itinerant degree of freedom and "localized-spin" degree of freedom become apparent and interact with each other. The physical ground of such a picture is attributed to the fact that the one-particle spectral weight has triple peak structure in strongly correlated fermion systems in general and large amount of the spectral weight is transferred to the high energy incoherent part while that of the coherent one decreases with the absolute value at the Fermi level unchanged. The triple peak structure consist of two broad peaks corresponding to the upper and lower Hubbard bands[10] and the narrow quasiparticle peak of Fermi liquid accessible by Gutzwiller's type description.[11] It has been explicitly recognized by Kawabata[12] two decade ago and demonstrated by recent numerical works with d=∞ technique, d being the space dimension.[13,14,15,16,17].

The incoherent part has influence on the physical quantities of the systems even in the low energy region where the Fermi liquid description is valid. In particular, the spin fluctuation spectrum is affected considerably by the incoherent part, or "localized spins", through a diffusive motion of clusters of "localized spins" with short range antifferomagnetic order. This is a salient nature of the duality model distinguished from a simple Fermi liquid description where the incoherent part is considered to be a simple featureless back ground. A possible importance of the incoherent parts was recognized by Ruckenstein and Varma[18] in the argument for a microscopic basis of the marginal Fermi liquid. We here retain the incoherent part explicitly as a "localized spin" degree of freedom which is the irrelevant operator that should be renormalized into the vertex part of the itinerant fermion at the fixed point.

In this paper, we present a microscopic justification of the duality model action for the Hubbard model with strong correlation on the basis of the renormalized perturbation expansion of the Luttinger-Ward skeleton representation for the thermodynamic potential. In this process, we make explicit use of the triple peak structure of the one-particle spectral weight. The organization of this paper is as follows. In §2 we develop a microscopic justification of the duality model action and in §3 we investigate the role of the high energy process on the fluctuations of the "localized spins" which have commensurate correlation through a superexchange-type interaction. Conclusion and discussion are given in §4.

§2. Justification of duality model - separation of itinerant and localized degree of freedom -

The effective action of the duality model for low energy physics of strongly correlated electron systems is written as [4)]

$$A = A_{\rm f} + A_{\rm s} + A_{\rm int}, \tag{2.1}$$

where

$$A_{\rm f} = -\sum_{i,j.\sigma}\sum_{n} f^{\dagger}_{i\sigma}(-{\rm i}\epsilon_n)(\bar{G}^{-1}_{ij,\sigma}({\rm i}\epsilon_n))f_{j\sigma}({\rm i}\epsilon_n), \tag{2.2a}$$

$$A_{\rm s} = \frac{1}{2}\sum_{i,j,m}\mathbf{S}_i(-{\rm i}\nu_m)(\chi^{-1}_{0ij}({\rm i}\nu_m))\mathbf{S}_j({\rm i}\nu_m), \tag{2.2b}$$

$$A_{\rm int} = -\lambda_0\sum_{i\alpha\beta}\sum_{mn} f^{\dagger}_{i\alpha}(-{\rm i}\epsilon_n - {\rm i}\nu_m)f_{i\beta}({\rm i}\epsilon_n)\sigma_{\alpha\beta}\cdot\mathbf{S}_i({\rm i}\nu_m), \tag{2.2c}$$

where $A_{\rm f}$ and $A_{\rm s}$ represent the parts of fermions and localized spin consisting of incoherent part of fermions respectively, and $A_{\rm int}$ is the interaction term of the fermion with the localized spin. The spin degree of freedom, $\mathbf{S}_i(\nu_m)$, mainly comes from the particle-hole exicitations with high energy part of fermions, corresponding to the Hubbard bands. However, energies ${\rm i}\nu_m$ of $\mathbf{S}_i$ are restricted essentially within the low-energy region comparable to the renormalized bandwidth of itinerant fermions. This is assumed by the structure of the dynamical susceptibility $\chi_{0ij}({\rm i}\nu_m)$ as the energies ${\rm i}\epsilon_n$ of fermions are restricted by the structure of $\bar{G}_{ij}({\rm i}\epsilon_n)$. It is also noted that $\mathbf{S}_i$ is a boson field describing the quantum fluctuation of the "localized spins" which has been almost quenched by high energy process such as the Kondo effect in Ce-based heavy fermions.

What we want to show below is that the action (2.1) is actually appropriate form for strongly correlated electron systems in the low energy region. If the renormalization-flow line of the original Hamiltonian of strongly correlated electron systems passes through the point where the duality model action can apply in the vicinity of the fixed point, then this duality action is a correct effective action of the original one. So we try to show that in the vicinity of the fixed point the renormalization drives the original Hamiltonian, which has strong on-site Coulomb interaction, toward the form of the duality model action.

A strategy we take here is to show that the thermodynamic potential in the duality model and that of the original Hamiltonian actually coincide with each other term by term under a certain condition satisfied by strongly correlated electron systems. The duality model is the effective model in the region where the renormalization has been carried out appreciably but not completely. So we take the Luttinger–Ward functional form which is the functional of the fully renormalized Green function and the self energy of the original Hamiltonian and expand it about the point corresponding to the duality model. The thermodynamic potential Y of the original Hamiltonian

of the Luttinger-Ward[19] form is

$$Y = T\sum_{\epsilon_n}\sum_{p,\sigma} e^{\mathrm{i}\epsilon_n\delta}[\ln G_\sigma(p,\mathrm{i}\epsilon_n) - \Sigma_\sigma(p,\mathrm{i}\epsilon_n)G_\sigma(p,\mathrm{i}\epsilon_n)] + \Phi[G_\sigma(p,\mathrm{i}\epsilon_n)], \tag{2.3}$$

where $G_\sigma(p,\mathrm{i}\epsilon_n)$ and $\Sigma_\sigma(p,\mathrm{i}\epsilon_n)$ is fully renormalized Green function and self energy respectively and $\Phi[G_\sigma(p,\mathrm{i}\epsilon_n)]$ is the Luttinger-Ward functinal defined by

$$\Phi[G_\sigma] = T\sum_{\epsilon_n}\sum_{p,\sigma}\sum_{n}\frac{1}{2n}\Sigma^n{}_\sigma(p,\mathrm{i}\epsilon_n)G_\sigma(p,\mathrm{i}\epsilon_n), \tag{2.4}$$

where $\Sigma^n{}_\sigma(p,\mathrm{i}\epsilon_n)$ is the n-th order contribution to the self energy from all the possible skeleton diagrams with the fully renormalized Green functions $G_\sigma(p,\mathrm{i}\epsilon_n)$. To avoid an overcounting of the same diagram composed of $2n$ Green function, the factor $\frac{1}{2n}$ appears in (2.4).

We show the expansion of the Luttinger-Ward functional $\Phi[G_\sigma]$ up to the 4th order term of the Hubbard model in Fig.[1], the solid line is the renormalized Green function and the dotted line is the bare Coulomb interaction U. In Fig.[2], on the other hand, we also show the expansion of thermodynamics potential Ω of the duality model up to 4th order of coupling constant λ_0. In Fig.[2], the solid line represents the Green function $\bar{G}_\sigma$ of the fermion of the duality model and the wavy line the propageter χ_0 of the "localized spin", and Ω_0 is the noninteracting part of the thermodynamical potential which is written as

$$\Omega_0 = T\sum_{\epsilon_n}\sum_{p,\sigma} e^{\mathrm{i}\delta\epsilon_n}\ln\bar{G}_\sigma(p,\mathrm{i}\epsilon_n). \tag{2.5}$$

If the expansion (2.3) of Y, the thermodynamic potential of the original Hamiltonian, is reduced to the expansion of Ω, that of the duality model, under a certain reasonable condition, we get the correctness of the duality model action (2.1) $\sim$ (2.4). To show the equivalence of the expansion Ω to Y, the diagrams of Y need to be reduced to those of Ω with correct coefficients of corresponding diagrams. The expansion of the thermodynamic potential Y contains the fully renormalized Green function G_σ which describes the physics around the fixed point. On the other hand, the expansion of Ω contains the Green function of duality model $\bar{G}_\sigma$ which is only partially renormalized. The fully renormalized Green function G is expanded as follow.

$$G_\sigma(p,\epsilon) = \tilde{G}_\sigma(p,\epsilon) + \delta G_\sigma(p,\epsilon), \tag{2.6}$$

where $\tilde{G}_\sigma(p,\epsilon)$ is the partially renormalized Green function appearing in the duality model action (2.2a) and $\delta G_\sigma(p,\epsilon)$ is the correction due to the renormalization by the interaction (2.2c). Here we set up following physical assumptions.

First we assume that in the energy region, where the duality model can apply, the coherent fermions interact only through the spin fluctuations because the charge fluctuations with high energy scale are suppressed in strongly correlated electron systems. The diagrams of $\delta G_\sigma(p,\mathrm{i}\epsilon_n)$ are

given as shown in Fig.[3] where the dotted line represents the partially renormalized Green function $\tilde{G}_\sigma(p, \mathrm{i}\epsilon_n)$ and the wavy line the spin fluctuations propagator χ_0 and the dot the fermion-spin vertex part λ_0.

Another and the most crucial assumption is that the one-particle spectral weight given by $\tilde{G}_\sigma$ already has the triple peak structure in the energy region in question. Namely, the quasi-particle peak is narrowed and considerable part of the spectral weight are transferred to the high energy region of upper and lower Hubbard band broad peak. The triple peak structure is a characteristic feature of the strongly correlated electron systems. Due to this structure we can explicitly distinguish the high energy processes of fermion excitations which belong to the incoherent parts of the upper and lower Hubbard bands and the low energy processes of fermions which belong to the coherent part of quasiparticles. The information that the electron system is in strongly correlated region is condensed to the explicit separation of high and low energy part of fermion excitations. We can assume this *a posteriori*.

Hereafter we consider the diagrammatic structures of the Green function $\tilde{G}_\sigma(p, \epsilon)$ and $\delta G_\sigma(p, \epsilon)$ in detail. The partially renormalized Green function $\tilde{G}_\sigma(p, \epsilon)$ is written as follow

$$\tilde{G}^{-1}{}_\sigma(p, \mathrm{i}\epsilon_n) = G^{-1}{}_{0\sigma}(p, \mathrm{i}\epsilon_n) - \tilde{\Sigma}_\sigma(p, \mathrm{i}\epsilon_n), \tag{2.7}$$

where $G_{0\sigma}(p, \mathrm{i}\epsilon_n)$ is the bare Green function and $\tilde{\Sigma}_\sigma(p, \mathrm{i}\epsilon_n)$ is a partially renormalized selfenergy which is composed only of high energy process. Here the one particle-spectrum, expressed by $\rho(x) = -\frac{1}{\pi}\mathrm{Im}\tilde{G}_\sigma(p, x)$, has triple peak structure already and the low energy coherent parts are narrowed while the high energy incoherent parts are broadened. We can separate the high energy incoherent process and the low energy coherent process in the spectral representation as

$$\begin{aligned}
\tilde{G}_\sigma(p, \mathrm{i}\epsilon_n) &= \int \mathrm{d}x \frac{\rho(x)}{x - \mathrm{i}\epsilon_n} && \text{(2.8a)} \\
&= \int \mathrm{d}x \frac{\rho_{\mathrm{H}}(x)}{x - \mathrm{i}\epsilon_n} + \int \mathrm{d}x \frac{\rho_{\mathrm{L}}(x)}{x - \mathrm{i}\epsilon_n} && \text{(2.8b)} \\
&\equiv \tilde{G}^{\mathrm{H}}{}_\sigma(p, \mathrm{i}\epsilon_n) + \tilde{G}^{\mathrm{L}}{}_\sigma(p, \mathrm{i}\epsilon_n). && \text{(2.8c)}
\end{aligned}$$

The $\rho_{\mathrm{H}}(x)$ is the incoherent part of the one particle spectral weight and the $\rho_{\mathrm{L}}(x)$ is the coherent one. The Green function $\tilde{G}^{\mathrm{H}}{}_\sigma(p, \mathrm{i}\epsilon_n)$ and the $\tilde{G}^{\mathrm{L}}{}_\sigma(p, \mathrm{i}\epsilon_n)$ are defined as

$$\begin{aligned}
\tilde{G}^{\mathrm{H}}{}_\sigma(p, \mathrm{i}\epsilon_n) &= \int \mathrm{d}x \frac{\rho_{\mathrm{H}}(x)}{x - \mathrm{i}\epsilon_n}, && \text{(2.9a)} \\
\tilde{G}^{\mathrm{L}}{}_\sigma(p, \mathrm{i}\epsilon_n) &= \int \mathrm{d}x \frac{\rho_{\mathrm{L}}(x)}{x - \mathrm{i}\epsilon_n} && \text{(2.9b)} \\
&= \frac{\tilde{z}}{\mathrm{i}\epsilon_n - \tilde{\xi}_p}, && \text{(2.9c)}
\end{aligned}$$

where $\tilde{z}$ is the renormalization factor of itinerant part of duality model, and is given as $\tilde{z} = (1 - \partial\tilde{\Sigma}(x)/\partial x)^{-1}$ and the $\tilde{\xi}_p$ is a partially renormalized dispersion. We note that the $\tilde{z}$ becomes

already small comparable to the order of z, the renormalization factor at the fixed point.

Now let us discuss a character of the spin fluctuations which are included in $\delta G_\sigma(p, \mathrm{i}\epsilon)$. Due to the above assumptions, the spin fluctuations, composed of the incoherent part $\tilde{G}^{\mathrm{H}}{}_\sigma(p, \mathrm{i}\epsilon)$, dominate in the energy region where the duality model can apply. The incoherent parts of fermion are included in the irrelevant operator in general. If our standing point is the fixed point of the renormalization, the irrelevant operators of the high energy process are renormalized into the vertex parts. However once we leave the fixed point, the irrelevant operators will appear no matter how small they are, and in strongly correlated electron systems the spin fluctuation processes will be the largest among such irrelevant operators. Considering the fact that the particle-hole excitation with high energy fermions can carry the low energy, the spin fluctuation process from the incoherent part play an appreciable role for the interaction between fermions due to the broad upper and the lower Hubbard bands. From the Ward-identity argument[4] about the strength of spin-fermion coupling for the impurity Anderson model, we can assume that fermions strongly interact with the "localized-spin". So the diagrams of δG in Fig.[3] can be regarded as we explicitly take out the irrelevant spin-fluctuation processes from the selfenergy and neglect other fermion processes owing to their relative smallness compared to the spin fluctuations.

By substituting the Green function G, (2.6), the thermodynamic potential Y, (2.3), can be rearranged as follows:

$$
\begin{aligned}
Y &= \ln G - \Sigma G + \Phi[G] && \text{(2.10a)}\\
&= \ln \tilde{G} && \text{(2.10b)}\\
&+ \ln(1 + \frac{\delta G}{\tilde{G}}) && \text{(2.10c)}\\
&- (\tilde{\Sigma} + \delta\Sigma)(\tilde{G} + \delta G) && \text{(2.10d)}\\
&+ \Phi[\tilde{G}_{\mathrm{H}}] + \frac{\delta\Phi}{\delta G}|_{G=\tilde{G}_{\mathrm{H}}}\delta' G + \frac{\delta^2\Phi}{\delta G_1 \delta G_2}|_{G=\tilde{G}_{\mathrm{H}}}\delta' G_1 \delta' G_2 + \cdots, && \text{(2.10e)}
\end{aligned}
$$

where $\delta' G \equiv \tilde{G}_{\mathrm{L}} + \delta G$, and the summation with respect to frequency, momentum and spin are abbreviated. The contribution $\delta\Sigma$ represents the excess renormalization on the basis of the duality model in which only $\tilde{\Sigma}$ has been taken into account.

The term (2.10b) can be decomposed as

$$
T\sum_{\epsilon_n} \ln \tilde{G}(\mathrm{i}\epsilon_n) = \int_{x\in \mathrm{H}} \frac{\mathrm{d}x}{2\pi} \mathrm{th}\frac{x}{2T} \tan^{-1}\frac{\mathrm{Im}\tilde{G}(x)}{\mathrm{Re}\tilde{G}(x)} + \int_{x\in \mathrm{L}} \frac{\mathrm{d}x}{2\pi} \mathrm{th}\frac{x}{2T} \tan^{-1}\frac{\mathrm{Im}\tilde{G}(x)}{\mathrm{Re}\tilde{G}(x)}, \qquad (2.11)
$$

where the symbol $x \in \mathrm{L}$ and $x \in \mathrm{H}$ mean that the region of integration is restricted to the low and high energy region, respectively. The second term of (2.11) includes only the low energy process and is equivalent to $\ln \tilde{G}_{\mathrm{L}}$ which corresponds to the thermodynamic potential Ω, (2.5), the non-interacting part of the duality model, if $\bar{G}$ is identified with $\tilde{G}_{\mathrm{L}}$.

The term (2.10-c) is further expanded as

$$\ln(1+\frac{\delta G}{\tilde{G}}) \simeq \sum_{n=1}^{\infty} \frac{(-1)^{n-1}}{n} (\frac{\delta G}{\tilde{G_{\rm L}}})^n. \tag{2.12}$$

where we have replaced $\tilde{G}$ by $\tilde{G}_{\rm L}$ in the right hand side because of the same reason as will be discussed below (2.14). The first and the second term of (2.12) are shown in Fig.[4].

We next rearrange the term (2.10-d) as

$$(\tilde{\Sigma}+\delta\Sigma)(\tilde{G}+\delta G) = \tilde{\Sigma}\tilde{G}_{\rm H} + \tilde{\Sigma}(\delta' G) + \delta\Sigma\tilde{G}_{\rm H} + \delta\Sigma\tilde{G}_{\rm L} + \delta\Sigma\delta G. \tag{2.13}$$

The third term of (2.13) is the convolution of $\delta\Sigma$ with the low energy components and with the $\tilde{G_{\rm H}}$ high energy ones, and is estimated as

$$T\sum_{\epsilon_n} \delta\Sigma({\rm i}\epsilon_n)\tilde{G}_{\rm H}({\rm i}\epsilon_n) = \int \frac{{\rm d}x}{\pi} \int \frac{{\rm d}x'}{\pi} \frac{{\rm Im}\delta\Sigma(x){\rm Im}\tilde{G}_{\rm H}(x')}{x-x'}[f(x)-f(x')], \tag{2.14}$$

where $f(x)$ is the Fermi distribution function. The integration value x belongs to the coherent low energy region and x' to the incoherent high energy region. Owing to the triple peak structure of one particle spectrum, the denominator $x-x'$ is roughly estimated about half of the on-site Coulomb energy U in the main contribution of the integral, so this term is negligible. The first term of (2.13) gives a constant in the sense of the duality model because it comes from the high energy processes.

Finally, we consider the term (2.10-e). Here the equality

$$\frac{\delta\Phi}{\delta G}|_{G=\tilde{G}_{\rm H}} = \tilde{\Sigma} \tag{2.15}$$

holds because of the property of the functional $\Phi[G]$, so that the second term of (2.10e) cancels with the second term of (2.13). The remaining terms of (2.13) are shown in Fig.[5]. The remaining terms of (2.10e) are obtained by replacing $\tilde{G}_{\rm H}$'s in the skeleton diagrams of $\Phi[G_H]$ with $\tilde{G}_{\rm L}$ or δG by the number of the order of functional derivative of $\Phi[G]$ in all possible ways. On replacing $\tilde{G}_{\rm H}$ of the $\Phi[G_{\rm H}]$ with $\tilde{G}_{\rm L}$ or δG, we select the diagrams which can contain the spin fluctuations made of $\tilde{G}_{\rm H}$, representing high energy process, and discard the diagrams from which we cannot extract the spin fluctuation process as irrelevant ones in the energy region where the duality model can be applied. For example, of the diagrams shown in Fig.[1] of $\Phi[G]$, c and f which contain only the singlet pair fluctuations are regarded as irrelevant ones and will be discarded. We assign the high energy incoherent part $\tilde{G}_{\rm H}$ for the spin fluctuation part of the diagrams of $\Phi[G]$ and the spin-fermion vertex parts which correspond to the coupling λ_0 of the duality model. The remaining part of the diagram consists of the low energy coherent part $\tilde{G}_{\rm L}$ or δG.

We illustrate the decomposition of the skeleton diagrams of $\Phi[G]$ up to the 4th order in U following the above mentioned procedure in Fig.[6], where the thick solid line and thin solid one represent $\tilde{G}_{\rm H}$, the high energy incoherent part, and $\tilde{G}_{\rm L}$, the low energy coherent part,respectively, and the

dotted line represents the bare Coulomb potential U, and the wavy line represents the spin fluctuation propagator χ_0 which represents the longitudinal part χ_0^z or the transverse part $\chi_0^{+-} = \chi_0^x + \chi_0^y$. In Fig.[7] we show the spin fluctuation propagator χ_0^z and χ_0^{+-} in terms of $\tilde{G}_{\rm H}$ up to the second order in U. We take up to the first correction of $\tilde{G}_{\rm L}$ by χ_0. This is consistent with retaining the terms up to the 4th order in U for $\Phi[G]$. The coefficients are attached to the diagrams in Fig.[6] because they are important when we compare with those corresponding to the expansion in the duality model. It is noted that the bubble of high energy component, in the second diagram of Fig.[6-a], includes both the charge susceptibility and the longitudinal spin susceptibility χ_0^z in this level of approximation. However, since the charge fluctuations are irrelevant here, the coefficient of χ_0^z should be assigned so as to maintain the isotropy in the spin space by comparing with the diagram containing the transverse susceptibility χ_0^{+-}, the first diagram of Fig.[6-a] for instance.

Here, as an example, we explain the diagrams derived from the $\frac{\delta^2\Phi}{\delta G_1 \delta G_2}|_{G=\tilde{G}_{\rm H}}\ \delta' G_1 \delta' G_2$ of the diagram g in Fig [6]. The diagrams (g-1) and (g-2) are included in the diagram A in the expansion of the duality model with the correct coefficient 1/2. Indeed, the diagram (g-1) can be regarded as a correction to the first term of Fig.[6-a] which contains the first term of χ_0 given in Fig.[7]. The diagram (g-2) contains the two equivalent diagrams which give corrections of two vertices of the first term of Fig.[6-a] because the diagram A in the duality model has the spin-fermion coupling λ_0 at both edges of the spin fluctuation χ_0. The diagrams (g-4) and (g-5) contain the first correction to those of (g-1) and (g-2) by the spin fluctuations included in δG. The diagram (g-5) has two equivalent diagrams due to the same reason as for the diagram (g-2).

Thus the diagrams, derived from the diagrams of Fig.[1-a $\sim$ h] for $\Phi[G]$ by the procedure $\frac{\delta^2\Phi}{\delta G_1 \delta G_2}|_{G=\tilde{G}_{\rm H}} \delta' G_1 \delta' G_2$, can be rearranged into the diagrams A,B,C and D of Fig.[2] in the duality model with the coefficient 1/2, 1, 1/4 and 1/4, respectively. Half of the term corresponding to the diagram B cancels with the diagrams of Fig.[4] and Fig.[5]. Indeed, when we sum up the diagrams in Fig.[4] $\sim$ [5], corresponding to the terms (2.12) and (2.13) without the second term, up to the 4th order in the coupling λ_0, we are left with the diagram the same as B of the duality model with a coefficient $-1/2$. So after all we can reproduce the expansion of the thermodynamic potential in the duality model, shown in Fig.[2] up to the 4th order perturbation in the spin-fermion coupling. This kind of comparison can be extended to higher order perturbation without difficulty in principle. It is left for future investigations to show that the above correspondence between the duality model and the strongly correlated original Hamiltonian hold to all orders of skeleton expansion of $\Phi[G]$ in the intermediate stage of the renormalization.

In conclusion of this section, we have argued on the basis of the renormalized perturbation approach that the thermodynamic potential of the Hubbard model with strong correlation can be reduced to that of the itinerant-localized duality model. Although we have adopted the Hubbard model for conciseness of presentations, the argument can be extended without difficulty to other

models such as the periodic Anderson model.

§3. Spin-fluctuation propagator of "localized spin" exhibiting superexchange-type correlation

In this section we discuss a structure of the spin-fluctuation propagator $\chi_0(q,\omega)$ on the basis of an explicit calculation due to the 2nd order pertubation solution of the two-dimensional (2d) Hubbard model. The Hubbard Hamiltonian is written as

$$H=\sum_{k\sigma}\epsilon_k c^{\dagger}_{k\sigma}c_{k\sigma}+\frac{U}{N}\sum_{k,k'}\sum_{q(\neq 0)}c^{\dagger}_{k-q\uparrow}c^{\dagger}_{k'+q\downarrow}c_{k'\downarrow}c_{k\uparrow}, \tag{3.1}$$

where the conventional notations are used and N is the number of site. The explicit form of the one-particle energy ϵ_k is given by means of the hopping term $-t/2$ between the nearest-neighbor sites as

$$\epsilon_k=-t(\cos k_x a+\cos k_y a), \tag{3.2}$$

where a is the lattice constant. It is noted that the full bandwidth W is equal to $4t$.

The spin susceptibility $\chi_0(q,\mathrm{i}\omega_m)$ arising from the high energy processes is decomposed formally as

$${\chi_0}^{-1}(q,\mathrm{i}\omega_m)=\chi^{-1}(\mathrm{i}\omega_m)-J(q,\mathrm{i}\omega_m), \tag{3.3}$$

where $\chi(\mathrm{i}\omega_m)$ represents the one-site effect and $J(q,\mathrm{i}\omega_m)$ intersite effect among the "localized-spin" degrees of freedom. If $\chi_0(q,\mathrm{i}\omega_m)$ has a peak at the wavevector $Q=(\pi/a,\pi/a)$, it means that the nearest neighbor interaction is dominant. By investigating a U-dependence of the peak height of $\chi_0(q,0)$, we can obtain a physical picture for the interaction between the "localized spins". If $J(Q)$ scales as $1/U$ in the limit $U/W\gg 1$, we can conclude that it can be regarded as the superexchange interaction.

In deriving the duality model in the previous section we have set an important assumption that the one particle spectral weight has the triple peak structure. Therefore we have to calculate $\chi_0(q,\mathrm{i}\omega_m)$, due to the high energy incoherent part, by means of the Green functions which give the triple peak structure to the one particle spectrum. It is well known that the 2nd order perturbation with respect to U reproduces the triple peaks structure. So we use the 2nd order perturbed Green function $G^{(2)}(p,\mathrm{i}\epsilon_n)$, which includes the 2nd order perturbed selfenergy $\Sigma^{(2)}(p,\mathrm{i}\epsilon_n)$ as an approximate Green function leading to the duality model. We further approximate χ_0 as the first term shown in Fig.7. Namely, we take only the bubble diagram composed of $G^{(2)}_{\mathrm{H}}(p,\mathrm{i}\epsilon_n)$, the incoherent part of $G^{(2)}(p,\mathrm{i}\epsilon_n)$. The resultant structure of χ_0 will be compared with the approximate form of the full susceptibility χ_s calculated in the same way but with the use of $G^{(2)}$ which contains the low energy contributions as well.

In order to take out precisely the high energy part of the Green function, we perform the calculation on the real frequency axis. The retarded selfenergy as a function of the coordinate R and the time t in the 2nd order perturbation with respect to U is given as[21)]

$$\Sigma^{(2)}(R,t) = \frac{1}{\mathrm{i}} U^2 [a^2(R,t)b(R,t) + a(R,t)b^2(R,t)], \tag{3.4}$$

where the function $a(R,t)$ and $b(R,t)$ are defined as

$$a(R,t) = \frac{1}{N}\sum_p \mathrm{e}^{\mathrm{i}(p\cdot R - \xi_p t)} f(\xi_p), \tag{3.5a}$$

$$b(R,t) = \frac{1}{N}\sum_p \mathrm{e}^{\mathrm{i}(p\cdot R - \xi_p t)} [1 - f(\xi_p)], \tag{3.5b}$$

where $\xi_p \equiv \epsilon_p - \mu$, μ being the chemical potential, and $f(\xi_p)$ is the Fermi function. The function $a(R,t)$ and $b(R,t)$ can be calculated quickly by the fast Fourier transformation (FFT) algorithm. The selfenergy in the energy-momentum representation is given by

$$\Sigma(p,\omega) = \int_0^\infty \mathrm{d}t \mathrm{e}^{\mathrm{i}\omega t} \sum_R e^{-\mathrm{i}p\cdot R} \Sigma^{(2)}(R,t), \tag{3.6}$$

where both the time integration and the momentum summation are calculated by FFT. The calculations are performed with 128×128 sites. We introduce the upper cut-off Λ for the time integral and perform FFT in the interval $[0,\Lambda]$ with equally time spaced $N_e = 1024$ points. The cut-off Λ restricts the energy interval to the region $[-D, D]$, where $D = \pi N_e/\Lambda$, and we set Λ so as to $D = 5W = 20t$

The chemical potential μ is determined through the relation

$$n = \frac{1}{N}\sum_p \int \mathrm{d}\epsilon \rho^{(2)}(p,\epsilon) f(\epsilon), \tag{3.7}$$

where n is the electron number density per site and $\rho^{(2)}(p,\epsilon)$ is the spectral weight defined as

$$\begin{aligned} \rho^{(2)}(p,\epsilon) &\equiv -\frac{1}{\pi}\mathrm{Im}G^{(2)}(p,\epsilon) \\ &= -\frac{1}{\pi}\frac{\mathrm{Im}\Sigma^{(2)}(p,\epsilon)}{[\epsilon - \mu - \mathrm{Re}\Sigma^{(2)}(p,\epsilon)]^2 + [\mathrm{Im}\Sigma^{(2)}(p,\epsilon)]^2}. \end{aligned} \tag{3.8}$$

In Fig[8a] and [8b] we show the calculated results of the one-particle spectral weight of the systems with $n = 1.0$ and $n = 0.7$, respectively, for various values of U/W. When the Coulomb interaction U is comparable with the bandwidth W, the one particle spectrum gets the lower and upper Hubbard bands and becomes the triple peak structure, and exhibits the narrowing of the coherent peak with increasing U.

We first calculate $\chi_s(q,\omega)$, since its calculation is simpler than that of $\chi_0(q,\omega)$ where the low energy processes should be excluded. The approximate form of $\chi_s(q,\omega)$ given by bubble diagram is calculated by means of $G^{(2)}(p,\epsilon)$ as

$$\chi_s(q,\omega) = i\sum_k \int_0^\infty \mathrm{d}t \mathrm{e}^{\mathrm{i}\omega(t+\delta)} [X^*{}_{k+q}(t)Y_k(t) - Y^*{}_{k+q}(t)X_k(t)]. \tag{3.9}$$

where δ is a positive infinitesimal and the function $X_k(t)$ and $Y_k(t)$ are defined as

$$X_k(t) \equiv \int \mathrm{d}\epsilon \mathrm{e}^{\mathrm{i}t\epsilon}\rho^{(2)}(k,\epsilon), \tag{3.10}$$

$$Y_k(t) \equiv \int \mathrm{d}\epsilon \mathrm{e}^{\mathrm{i}t\epsilon}\rho^{(2)}(k,\epsilon)f(\epsilon). \tag{3.11}$$

The expression (3.9) is the convolution form of $X_k(t)$ and $Y_k(t)$ in the momentum space so that it can be calculated quickly by FFT. The calculation is performed at low enough temperature T=0.01t=0.0025$\,W$.

The momentum dependence of the approximate full susceptibility $\chi_s(p,\omega)$ for $\omega = 0$ is shown in Fig[9a], [9b] and [9c] for various fillings. The incommensurate peaks can be seen for all value of U/W in the case of filling n=0.7 (Fig[9c]), while they lose their height with increasing the ratio of U/W. In the case n=0.8, the incommensurate peaks disappear even for U/W=1.0. In these figures the incommensurate peaks appear in rather large doping for large U/W. This is the effect of the approximation that we take but there is a physical reason that the coherent peak which gives the incommensurate peak in the susceptibility is narrowed and its weight shifts to the high energy incoherent part which is the localized component, so the incommensurate peaks tend to vanish in strong Coulomb potential U. We also see that the value of susceptibility decreases with increasing U. We explain these below with paying attention to the role of incoherent lower and upper Hub bard bands.

Next we calculate the susceptibility $\chi_0(q,\mathrm{i}\omega_m)$ which is determined only by G_{H}'s representing the high energy processes. So, we need an explicit form of G_{H}. For constructing the Green function G_{H}, we introduce the cut-off which separates the low energy coherent peak and the high energy Hubbard bands. Of course the one particle spectrum of the Green function must be the triple peak structure for getting such cut-off.

Here we give G_{H} as

$$G_{\mathrm{H}}(p,\mathrm{i}\epsilon_n) = \int \mathrm{d}x \frac{\rho_{\mathrm{H}}(p,x)}{x - \mathrm{i}\epsilon_n}, \tag{3.12}$$

where $\rho_{\mathrm{H}}(p,x)$ is

$$\rho_{\mathrm{H}}(p,x) = \rho(p,x)g(x,c_1,c_2), \tag{3.13}$$

where $\rho(p,x)$ is usual one-particle spectral function, $-\frac{1}{\pi}\mathrm{Im}G(p,x)$, and the function $g(x,c_1,c_2)$ is the cut-off function which cuts the weight of the low energy coherent part that locating in the energy region $[c_1,c_2]$ as

$$g(x,c_1,c_2) = 1 + \frac{1}{\mathrm{e}^{\Gamma(x-c_1)}+1} - \frac{1}{\mathrm{e}^{\Gamma(x-c_2)}+1}, \tag{3.14}$$

where the Γ is a cut-off parameter and we set $\Gamma = 5t$. In order to decide the values c_1 and c_2, we select the saddle points between the the Hubbard peak and the coherent peak. In Fig[10]

we show the $\rho_{\rm H}(x) = \sum_p \rho_{\rm H}(p,x)$ for the half filled (a) and the $n = 0.7$ (b) case together with $\rho(x) = \sum_p \rho(p,x)$.

We give $\chi_0(q, {\rm i}\omega_m)$ the susceptibility of the incoherent part as

$$\chi_0(q, {\rm i}\omega_m) = -T \sum_{\epsilon_n} \sum_k G_{\rm H}(k+q, {\rm i}\epsilon_n + {\rm i}\omega_m) G_{\rm H}(k, {\rm i}\epsilon_n) \tag{3.15}$$

$$= \sum_k \int {\rm d}x \int {\rm d}x' \frac{\rho_{\rm H}(k+q,x)\rho_{\rm H}(k,x')}{{\rm i}\omega_m + x' - x} [f(x) - f(x')]. \tag{3.16}$$

Non-zero contributions to $\chi_0(q, {\rm i}\omega_m)$ arise from the integration regions of x and x' where x belongs to the upper Hubbard band and x' to the lower one, or vice versa, because the temperatures in question are low enough compared to the energy cut-off separating the coherent and incoherent parts. Then we can roughly estimate the denominator ${\rm i}\omega_m + x' - x$ in (3.16) for low temperature as $1/U$ and the difference of two Fermi distributions as ± 1. This seems to give t^2/U expected for the superexchange interaction. Unfortunately we cannot get the explicit $1/U$ scaling for the peak height of $\chi_0(q,0)$ in our approximation, although $\chi_0(Q,0)$ is a decreasing function of U in consistent with a general trend expected from the expression (3.16).

In Fig.[11a] we show the susceptibility of the incoherent parts $\chi_0(q,0)$, (3.16), for n=0.7 and U/W=1.0. It is noted that the peak of of $\chi_0(q,0)$ is located at commensurate position $Q = (\pi/a, \pi/a)$. This means that the spin degrees of freedom from the incoherent parts interact most strongly between nearest neighbor sites. The same point of view about the superexchange interaction was suggested by Ohkawa *et al.*[22] on the basis of the *1/d* expansion and rather rough estimate of the incoherent parts. In our approximation scheme it is apparent that the superexchange-type interaction is derived through the electron-hole pair excitations between the lower and upper Hubbard bands. The spin susceptibility $\chi_0(q,\omega)$ appearing in the duality model contains this information.

In Fig.[11b], we show the q-dependence of the full susceptibility $\chi_{\rm s}(q,0)$ calculated by (3.9). It is noted that the peak of $\chi_{\rm s}(q,0)$ is located at the incommensurate position. This is due to the effect of coherent motion of quasiparticle component which reflects the shape of the Fermi surface. It is a general characteristic of the duality description that the susceptibility $\chi_0(q)$, composed of the incoherent component, has commensurate correlation while the full susceptibility $\chi_{\rm s}(q)$, taking into account the coupling with the fermions, has the incommensurate correlation in general. Indeed the full dynamical spin fluctuation propagator in the duality model is formally written as

$${\chi_s}^{-1}(q, {\rm i}\omega_m) = {\chi_0}^{-1}(q, {\rm i}\omega_m) - {\lambda_0}^2 \Pi(q, {\rm i}\omega_m), \tag{3.17}$$

where the polarization $\Pi(q, {\rm i}\omega_m)$ of the fermion component is given by

$$\Pi(q, {\rm i}\omega_m) = -T \sum_{\epsilon_n p} \tilde{G}_{\rm L}(q+p, {\rm i}\omega_m + {\rm i}\epsilon_n) \tilde{G}_{\rm L}(p, {\rm i}\epsilon_n). \tag{3.18}$$

Then $\chi_s(q, \mathrm{i}\omega_m)$ exhibits peaks at incomensurate positions in general, reflecting the q-dependence of the polarization $\Pi(q, \mathrm{i}\omega_m)$.

It is noted that the incommensurate correlation of $\chi_{\mathrm{s}}(q, \omega)$ disappears as the frequency ω exceed the cut-off, separating the coherent and incoherent components, leaving only the commensurate correlation due to $\chi_0(q, \omega)$. Such a behavior has been recently discovered in by neutron scattering in Cr,[23] and will be discussed in detail elsewhere.

§4. Conclusion and discussion

In this paper we have examined the duality picture diagramatically and the origin of the superexchange interaction as electron hole pairs excitation between lower and upper Hubbard bands. The central assumption about the justification of the duality model is that in the intermediate stage of the renormalization, where the duality model can be applied, the one particle spectrum already have the triple peak structure and the spin fluctuation process from the incoherent parts is relatively larger than other processes, for example than the charge fluctuation. Due to the explicit separation between the incoherent/localized and coherent/itinerant parts we obtain naturally the "localized-spin" degree of freedoms with neglecting the other fluctuation freedoms. Here a question arises whether we can actually separate the coherent and incoherent parts so explicitly. In the impurity model like Anderson model and in the $d = \infty$ lattice model, d being the space dimension, which is equivalent to the impurity model under some conditions the coherent peak of the one particle spectrum is narrowed exponentially and the lower and upper Hubbard bands is developed explicitly with increasing the on site Coulomb U, we can safely set the above assumption. In the $d = 2$ and $d = 3$ lattice systems case like Hubbard model, the separation of the coherent and incoherent parts is not so clear as in the impurity cases. But we believe the duality model can apply to these cases as an effective action when the electron correlation is so strong.

In §2 we treat the fixed point just like as Fermi liquid but the same procedure is applicable for the non-Fermi liquid fixed point if the assumptions we mentioned are satisfied and there no singularity appears from the diagrams which we neglected. Actually we do not know the correct analytic form of the partially renormalized Green function $\tilde{G}(p, \mathrm{i}\epsilon_n)$ and the susceptibility of the localized spin $\chi_0(q, \mathrm{i}\omega_m)$, so we must input appropriate form of $\tilde{G}(p, \mathrm{i}\epsilon_n)$ and $\chi_0(q, \omega)$ which suitably describe the physical situation we deal. For example in the reference 5) $\sim$ 7) the weak antiferromagnatism of heavy fermion and the normal state properties of cupurate superconductor are successfully explained with the suitable form of $\tilde{G}(p, \mathrm{i}\epsilon_n)$ which include the nesting property. But by considering the structures of the incoherent part of fermions which are hidden, for example, in the Fermi Liquid theory we get the another properties and explanation of the strongly correlated fermion systems.

Acknowledgements

One of the authors (K.M.) has much benefitted from enlightening discussions with Y. Kuramoto at early stage of this work. This work is supported by the Grant-in-Aid for Scientific Research (07640477), and the Grand-in-Aid for Scientific Research on Priority Areas "Physics of Strongly Correlated Conductors" (06244104) and "Anomalous Metallic State near the Mott Transition" (07237102) from the Ministry of Education, Science, Sports and Culture.

[1] L. D. Landau: Sov. Phys. -JETP **3** (1957) 920.
[2] P. Nozières: J. Low Temp. Phys. **17** (1974) 32.
[3] K. Yamada and K. Yosida: Prog. Theor. Phys. **53** (1975) 1286.
[4] Y. Kuramoto and K. Miyake: J. Phys. Soc. Jpn. **59** (1990) 2831.
[5] Y. Kuramoto and K. Miyake: Prog. Theor. Phys. Suppl. **108** (1992) 199.
[6] K. Miyake and Y. Kuramoto: Physica B. **171** (1991) 20.
[7] K. Miyake and O. Narikiyo: J. Phys. Soc. Jpn. **63** (1994) 3821.
[8] O. Narikiyo and K. Miyake: J. Phys. Soc. Jpn. **63** (1994) 4169.
[9] O. Narikiyo: Physica C **267** (1996) 204.
[10] J. Hubbard: Proc. R. Soc. (London) A **276** (1963) 238; and *ibid.* A **281** (1964) 401.
[11] M. C. Gutzwiller: Phys. Rev. Lett. **10** (1963) 159.
[12] A. Kawabata: Prog. Theor. Phys. **54** (1975) 45.
[13] A. Georges and G. Kotliar: Phys. Rev. B **45** (1992) 6479.
[14] M. Jarrell: Phys. Rev. Lett. **69** (1992) 168.
[15] X. Y. Zhang, M. J. Rozenberg and G. Kotliar: Phys. Rev. Lett. **70** (1993) 1666
[16] Th. Pruschke, D. L. Cox and M. Jarrell: Phys. Rev. B **47** (1993) 3553
[17] O. Sakai and Y. Kuramoto: Solid State Commun. **89** (1994) 307.
[18] A. E. Ruckenstein and C. M. Varma: Physica C **185-189** (1991) 134.
[19] J. M. Luttinger and J. C. Ward: Phys. Rev. **119** (1960) 1417.
[20] P. W. Anderson: Phys. Rev. **115** (1959) 2.
[21] V. Zlatic, K.D.Schotte and G.Schiliecker: Phys. Rev. B. **52** (1995) 3639.
[22] F. J. Ohkawa and N. Matsumoto: J. Phys. Soc. Jpn. **63** (1993) 602.
[23] T. Fukuda, Y. Endoh, K. Yamada, M. Takeda, S. Itoh, M. Arai and T.Otomo: J. Phys. Soc. Jpn. **65** (1996) 1418.

Figure Captions

- Fig. [1]
  Diagrammatic expansion of the Luttinger-Ward functional $\Phi[G]$ up to the 4th order in the on-site Coulomb interaction. The solid line represents the fully renormalized Green function G and the dotted line the bare Coulomb interaction U. Summation of the momentum, frequency and spin index are abbreviated.

- Fig. [2]
  Diagrammatic expansion of the thermodynamic potential of the duality model. The solid line represents the partially renormalized Green function $\bar{G}$, and the wavy line the spin fluctuation propageter χ_0, and the dot the spin-fermion coupling λ_0.

- Fig. [3]
  Diagrammatic expression of $\delta G_\sigma(p, \mathrm{i}\epsilon_n)$. The wavy line represents χ_0 and the dot-dashed line represents $\tilde{G}_{\mathrm{L}}$, the dot is the spin-fermion vertex part which corresponds λ_0 of the duality model.

- Fig. [4]
  Diagrammatic expression of $(\delta G/\tilde{G})$ and $(\delta G/\tilde{G})^2$

- Fig. [5]
  Diagramatic expression of $(\delta\Sigma\tilde{G}_{\mathrm{L}} + \delta\Sigma\delta G)$ in (2.13).

- Fig. [6]
  Decomposition of the skeleton diagrams for the thermodynamic potential $\Phi[G]$ into the diagrams with high and low energy component. The thin line represents $\tilde{G}_{\mathrm{L}}$, the low energy part of the partially renormalized Green function and the thick line $\tilde{G}_{\mathrm{H}}$, the high energy one, and the dotted line the bare Coulomb interaction U. The symbol $\in$ means that the diagrams are included in the corresponding diagram (A $\sim$ D) of the duality model shown at the left side.

- Fig. [7]
  Diagrammatic expression of $\chi_0^z(q,\omega)$ and $\chi_0^{+-}(q,\omega)$. The solid line represents $\tilde{G}_{\mathrm{H}}$, the high energy part of the partially renormalized Green function, and the dotted line the bare Coulomb interaction U.

- Fig. [8]
  One-particle spectral weight $\sum_p \rho^{(2)}(p,\epsilon)$, given by (3.8), of the 2d Hubbard model for various values of U/W with the filling (a) n=1.0 and (b) n=0.7.

- Fig. [9]
  Wavevector dependence of the approximate full susceptibility $\chi_s(q,0)$ for various values of U/W. The filling are (a) n=1.0, (b) n=0.8, and (c) n=0.7, respectively.

- Fig. [10]
  One particle spectral weight $\rho_{\rm H}(\omega)$, the incoherent part which is indicated by the solid line, and $\rho^{(2)}(\omega) = \sum_p \rho^{(2)}(p,\omega)$, given by (3.8), which is indicated by the dotted line, for the case U/W=1.0. The fillings are (a) n=1.0 and (b) n=0.7

- Fig. [11]
  The wavevector dependence of (a) the susceptibility $\chi_0(q,0)$ of the incoherent part and (b) the full susceptibility $\chi_s(q,0)$ for the case U/W=1.0 and n=0.7

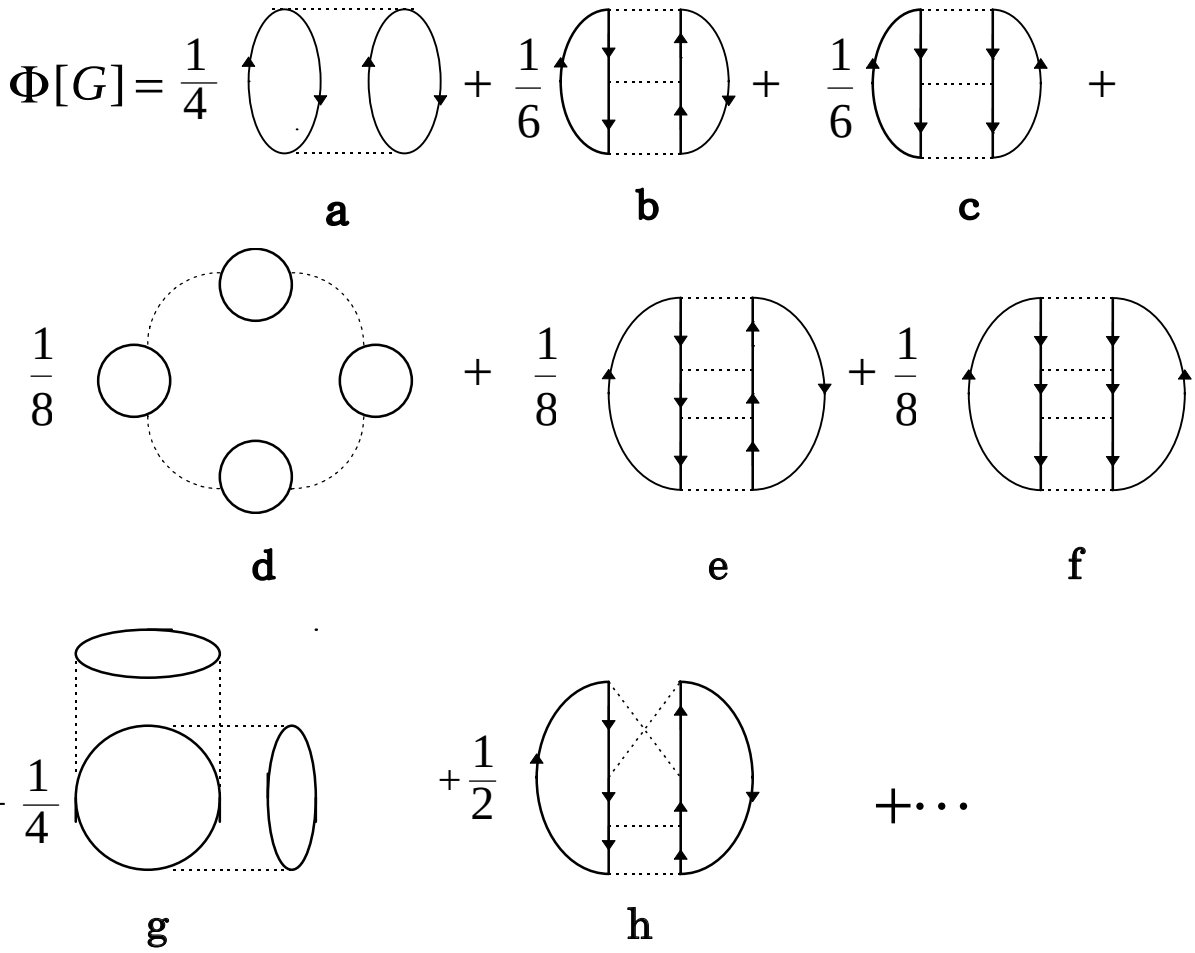
$\Phi[G] = \frac{1}{4}$
+
$\frac{1}{6}$
+
$\frac{1}{6}$
+
a
b
c
$\frac{1}{8}$
+
$\frac{1}{8}$
+
$\frac{1}{8}$
d
e
f
+ $\frac{1}{4}$
+ $\frac{1}{2}$
+ ⋯
g
h

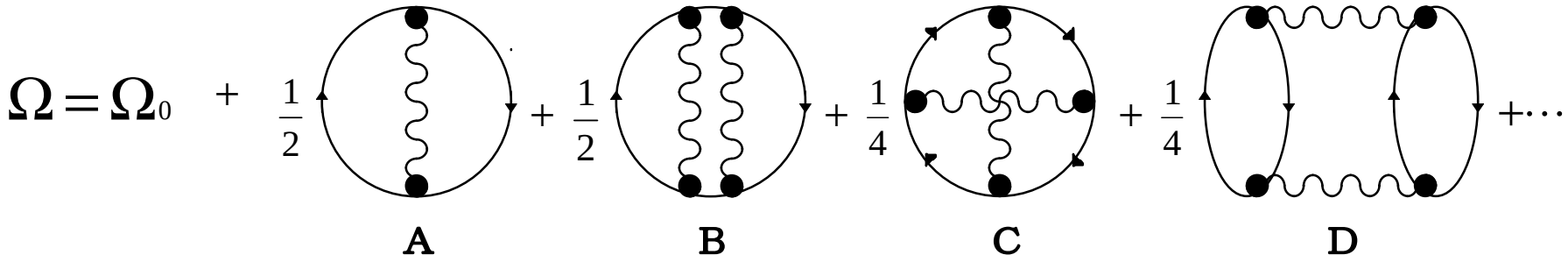
$\Omega = \Omega_0$ + $\frac{1}{2}$ + $\frac{1}{2}$ + $\frac{1}{4}$ + $\frac{1}{4}$ + ⋯
A
B
C
D

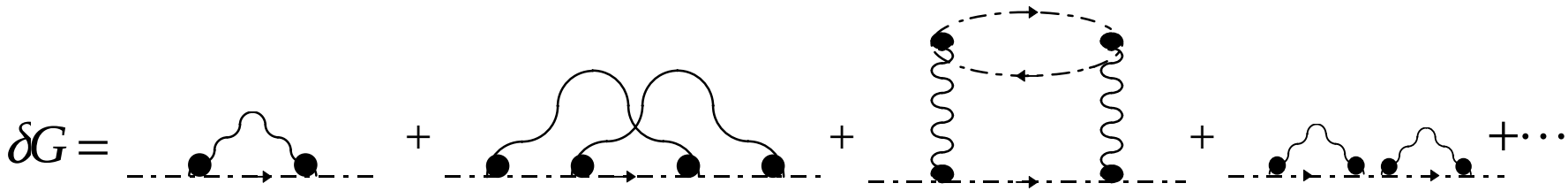
δG =
+
+
+
+⋯

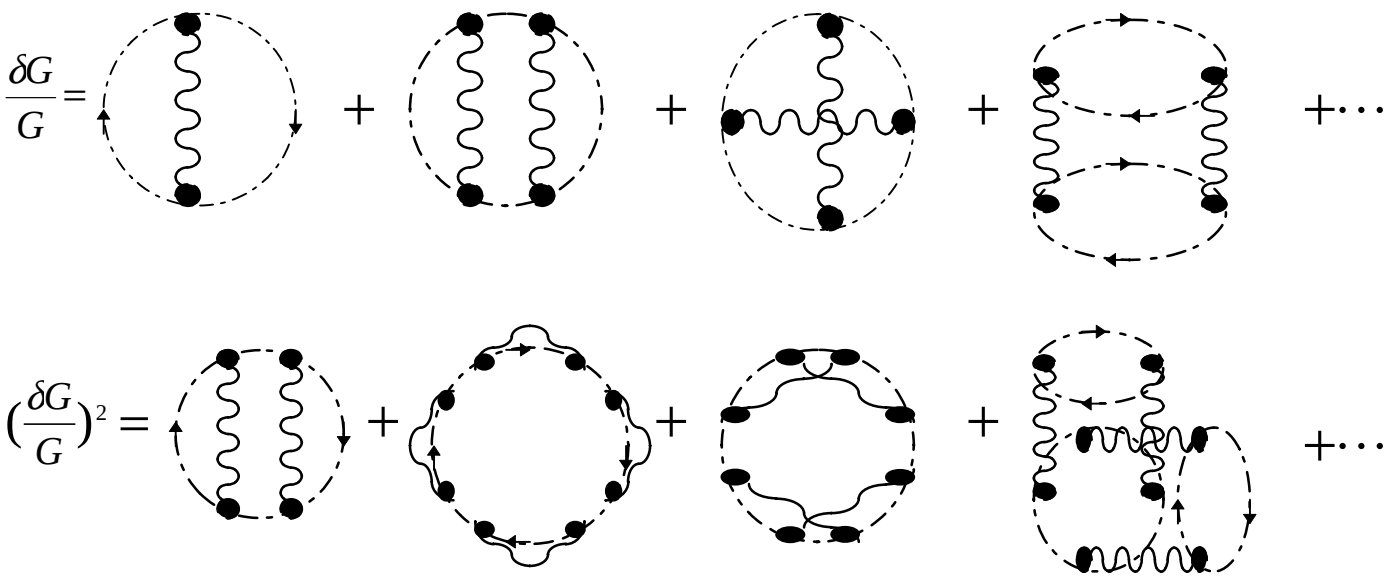

$$\delta\Sigma\overline{G}_L + \delta\Sigma\delta G =$$ 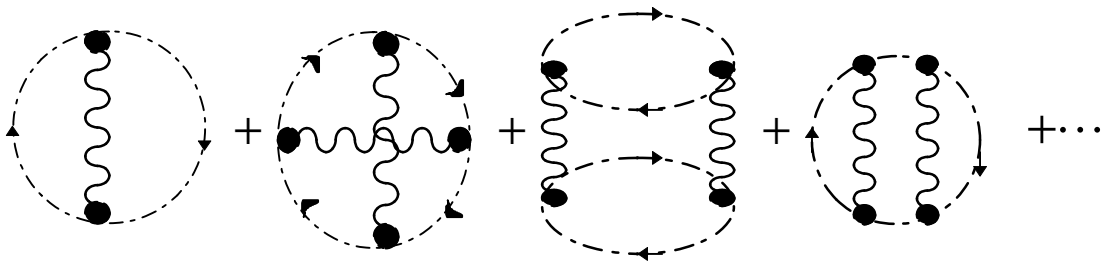 $$+\cdots$$

a)

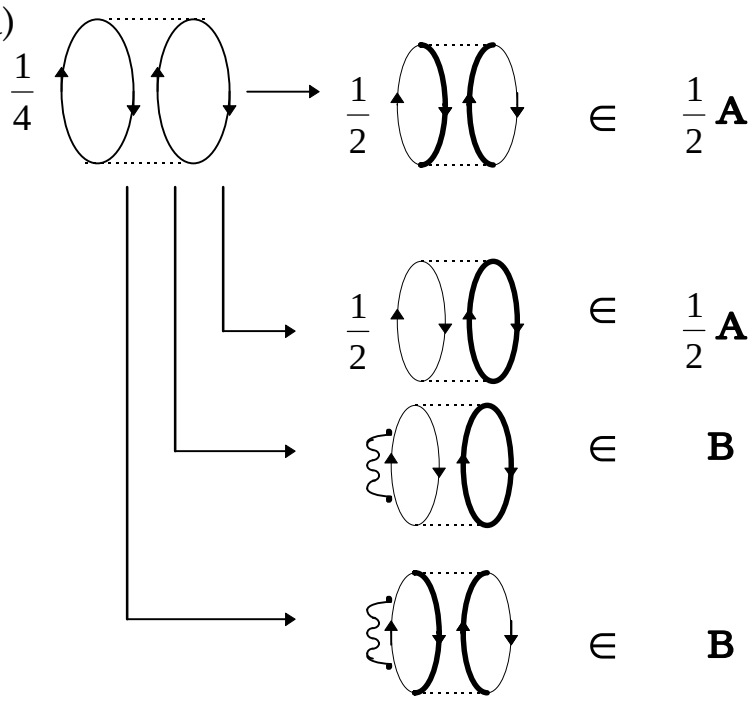

b)

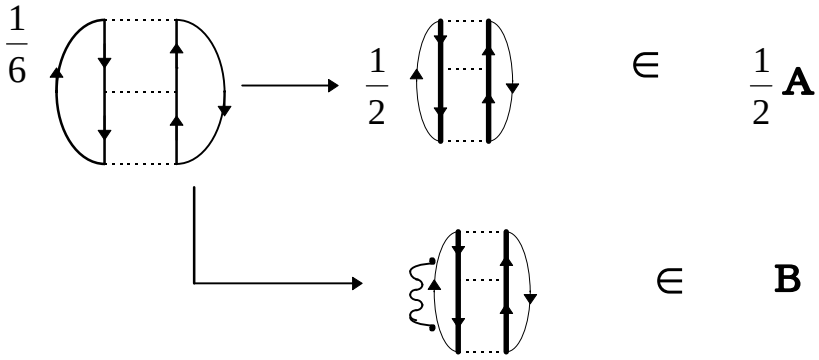

d)

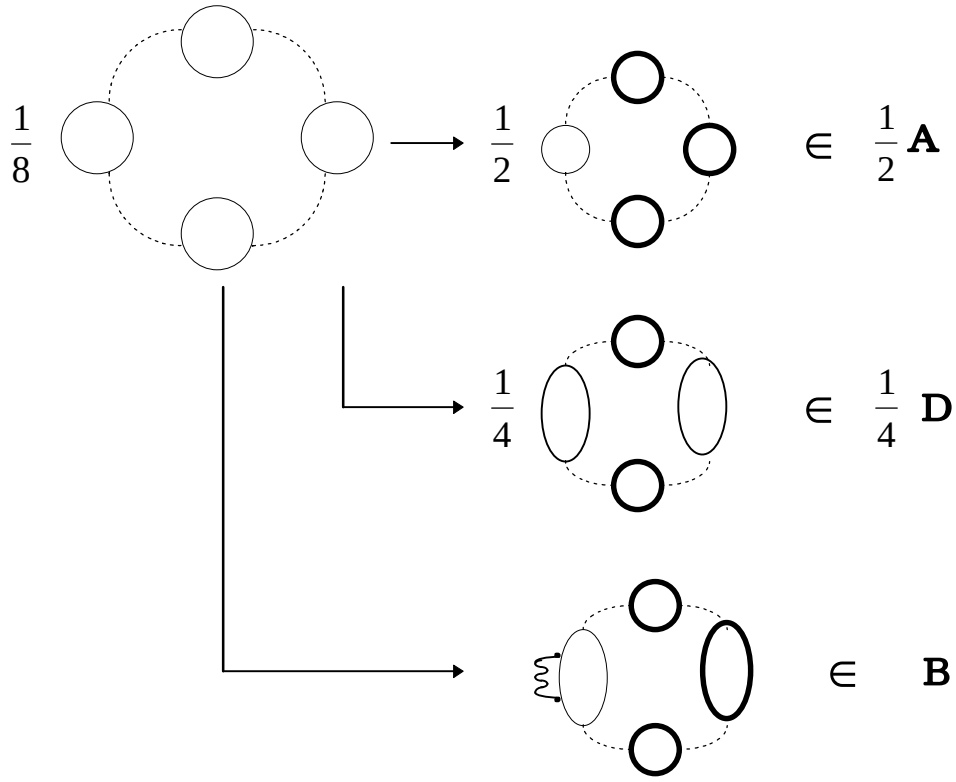

e)

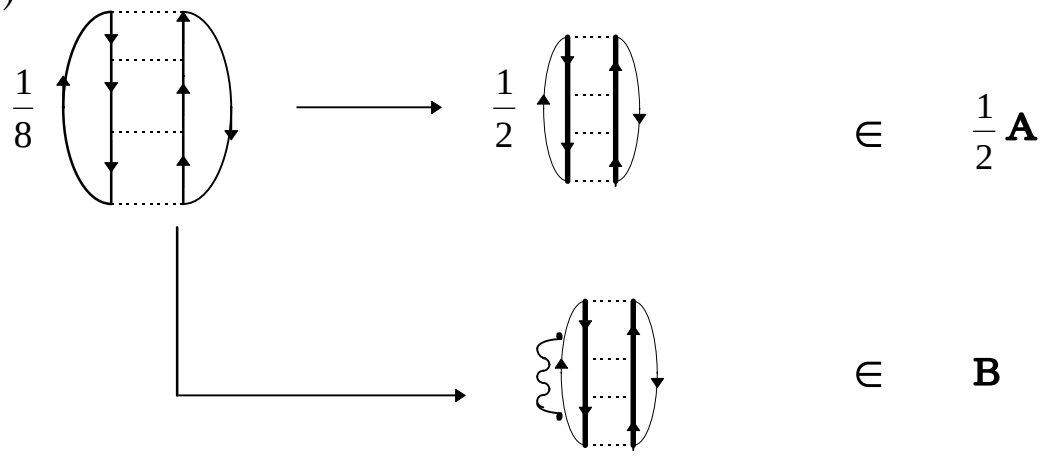

g)

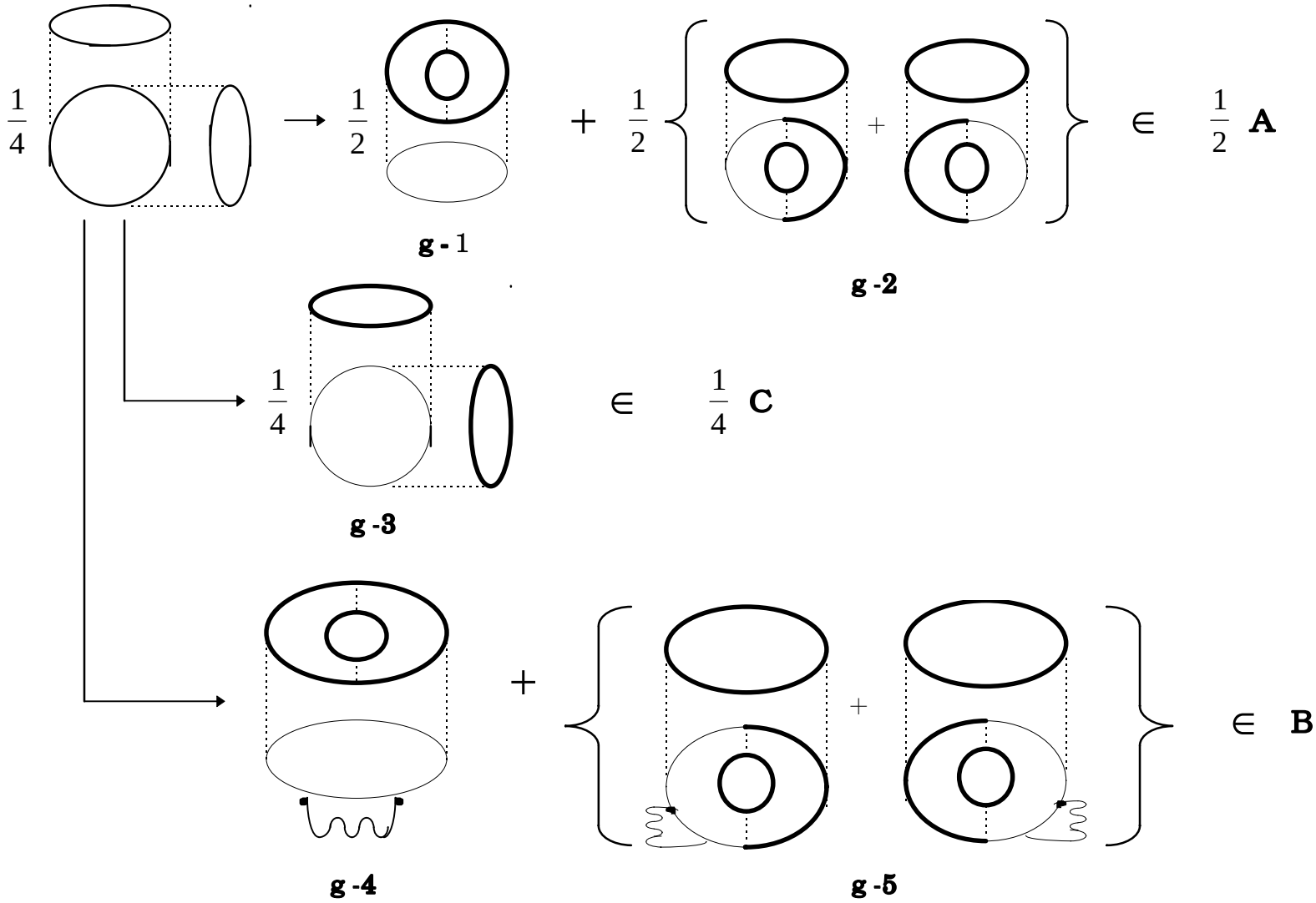

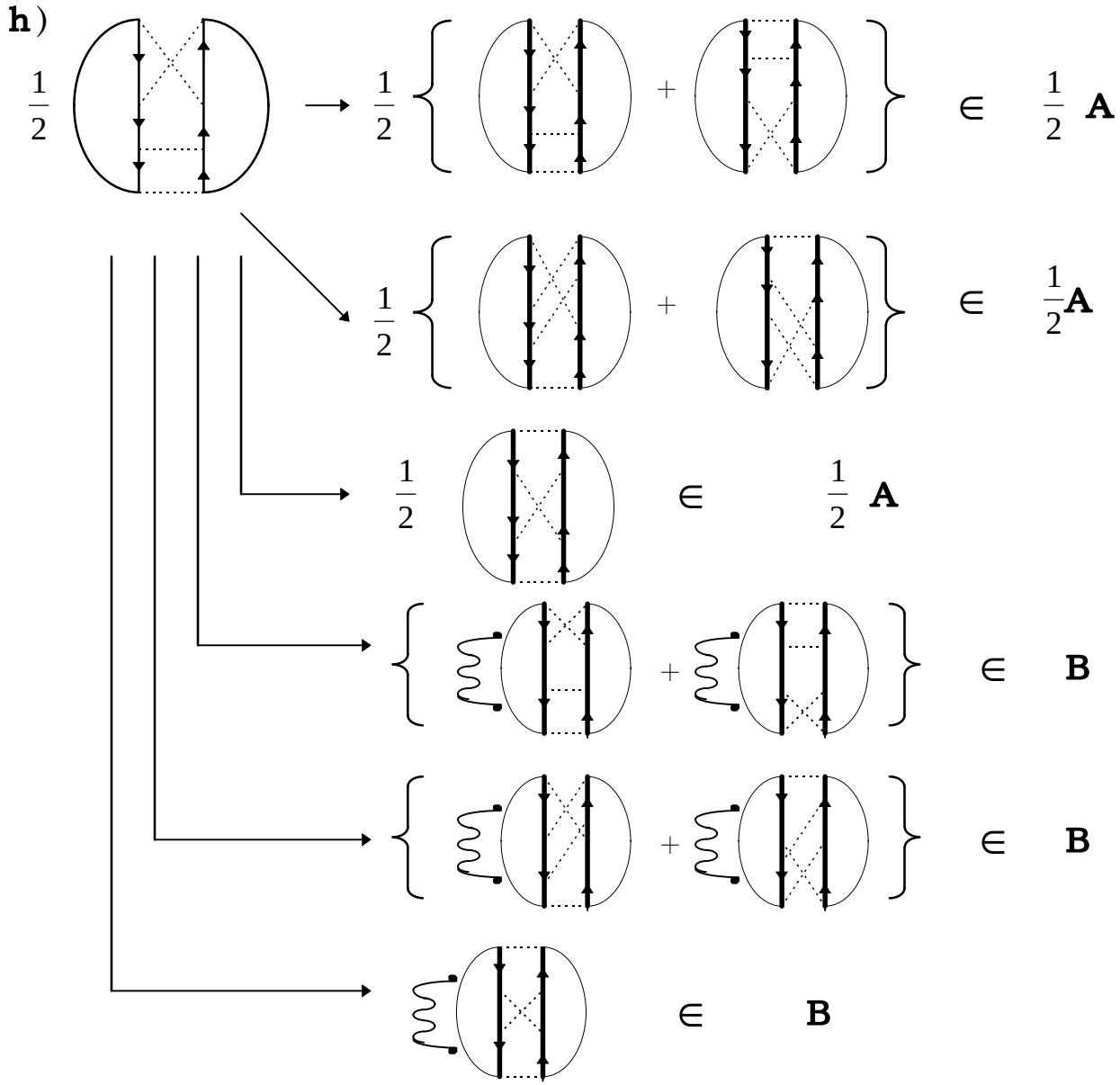
h)
1/2
1/2
+
∈
1/2 A
1/2
+
∈
1/2 A
1/2
∈
1/2 A
+
∈
B
+
∈
B
∈
B

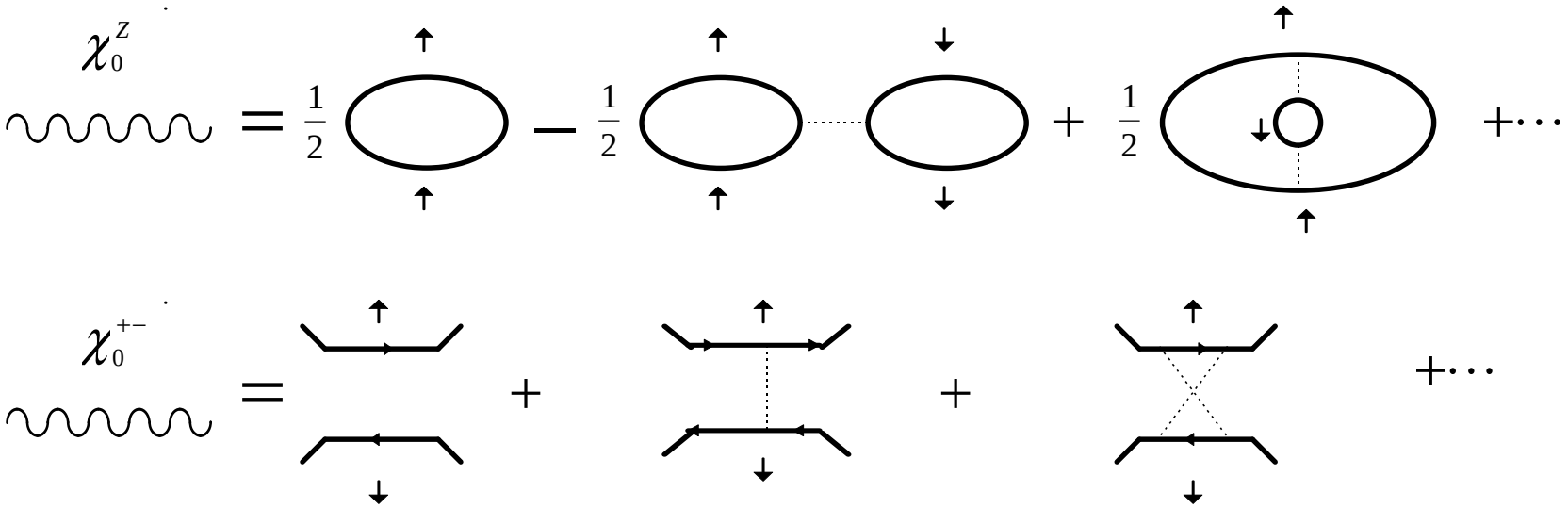
χ_0^Z
$= \frac{1}{2}$
$- \frac{1}{2}$
$+ \frac{1}{2}$
$+\cdots$
χ_0^{+-}
$=$
$+$
$+$
$+\cdots$

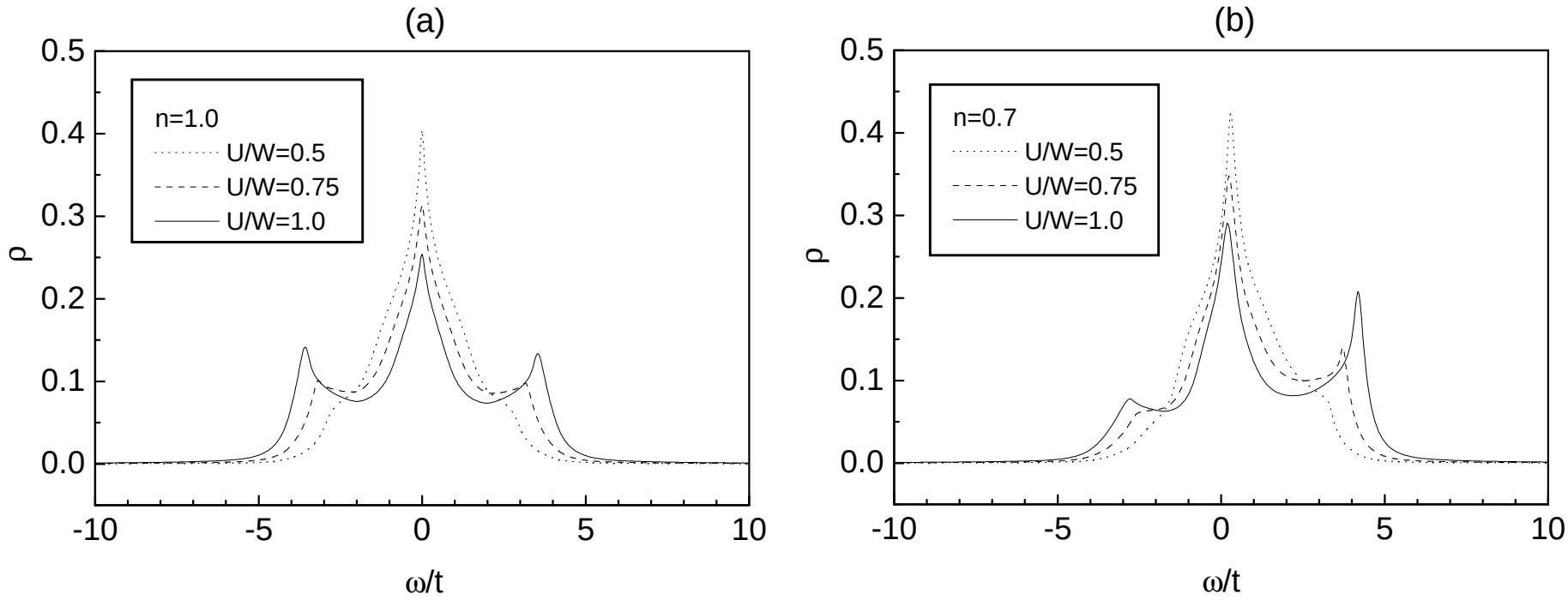
(a)
n=1.0
U/W=0.5
U/W=0.75
U/W=1.0
ρ
ω/t
(b)
n=0.7
U/W=0.5
U/W=0.75
U/W=1.0
ρ
ω/t

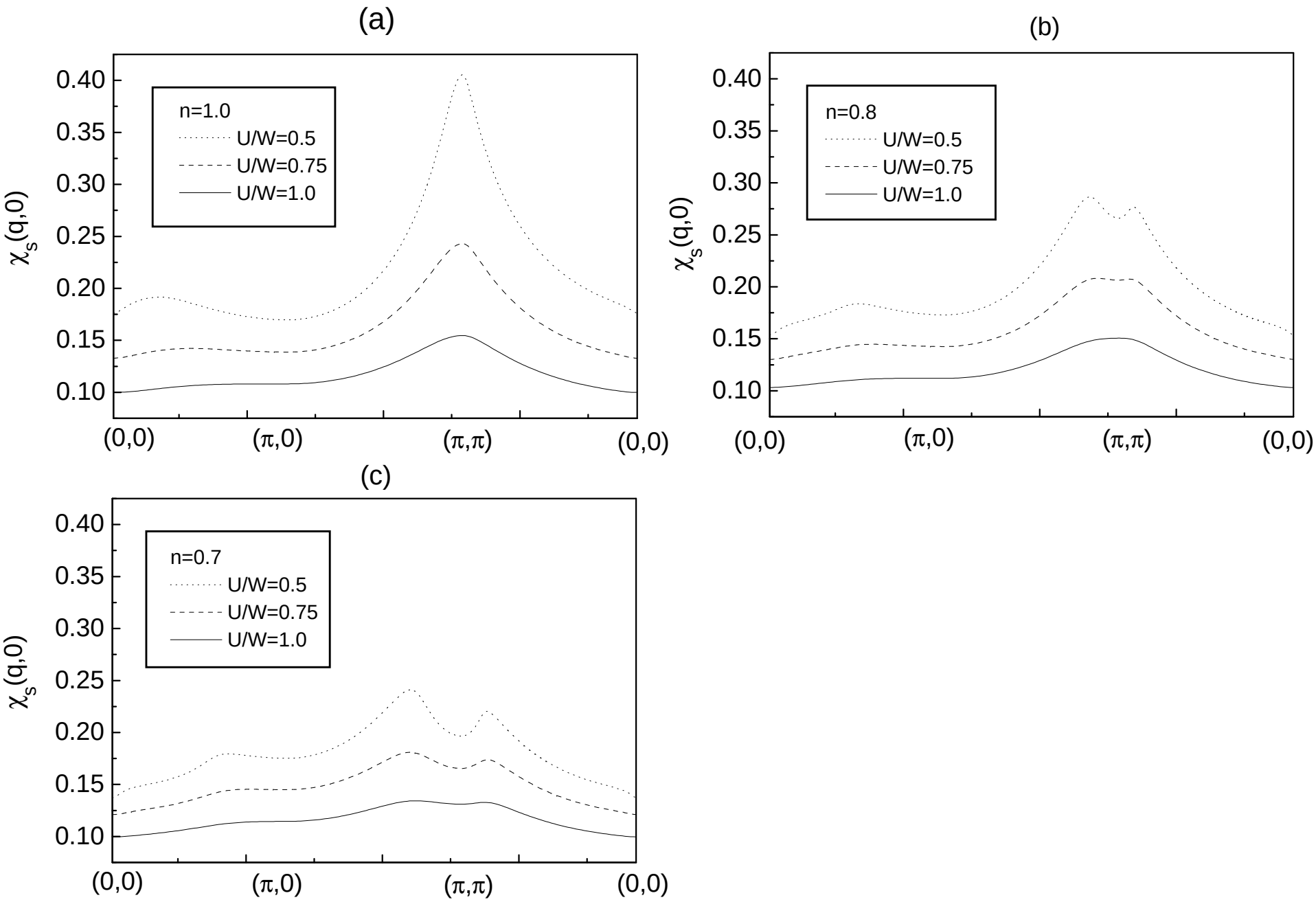
(a)
n=1.0
U/W=0.5
U/W=0.75
U/W=1.0
$\chi_s(q,0)$
0.40
0.35
0.30
0.25
0.20
0.15
0.10
(0,0)
(π,0)
(π,π)
(0,0)
(b)
n=0.8
U/W=0.5
U/W=0.75
U/W=1.0
$\chi_s(q,0)$
0.40
0.35
0.30
0.25
0.20
0.15
0.10
(0,0)
(π,0)
(π,π)
(0,0)
(c)
n=0.7
U/W=0.5
U/W=0.75
U/W=1.0
$\chi_s(q,0)$
0.40
0.35
0.30
0.25
0.20
0.15
0.10
(0,0)
(π,0)
(π,π)
(0,0)

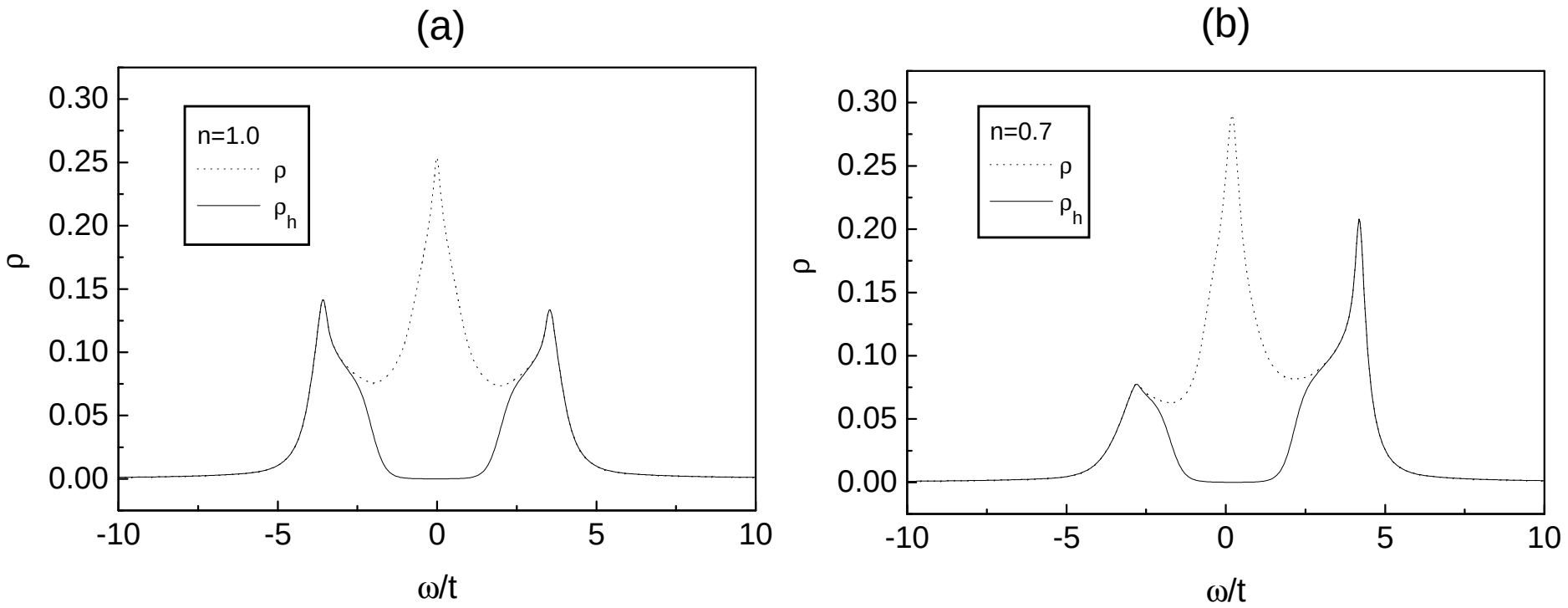
(a)
n=1.0
ρ
ρh
0.30
0.25
0.20
0.15
0.10
0.05
0.00
-10
-5
0
5
10
ω/t
(b)
n=0.7
ρ
ρh
0.30
0.25
0.20
0.15
0.10
0.05
0.00
-10
-5
0
5
10
ω/t

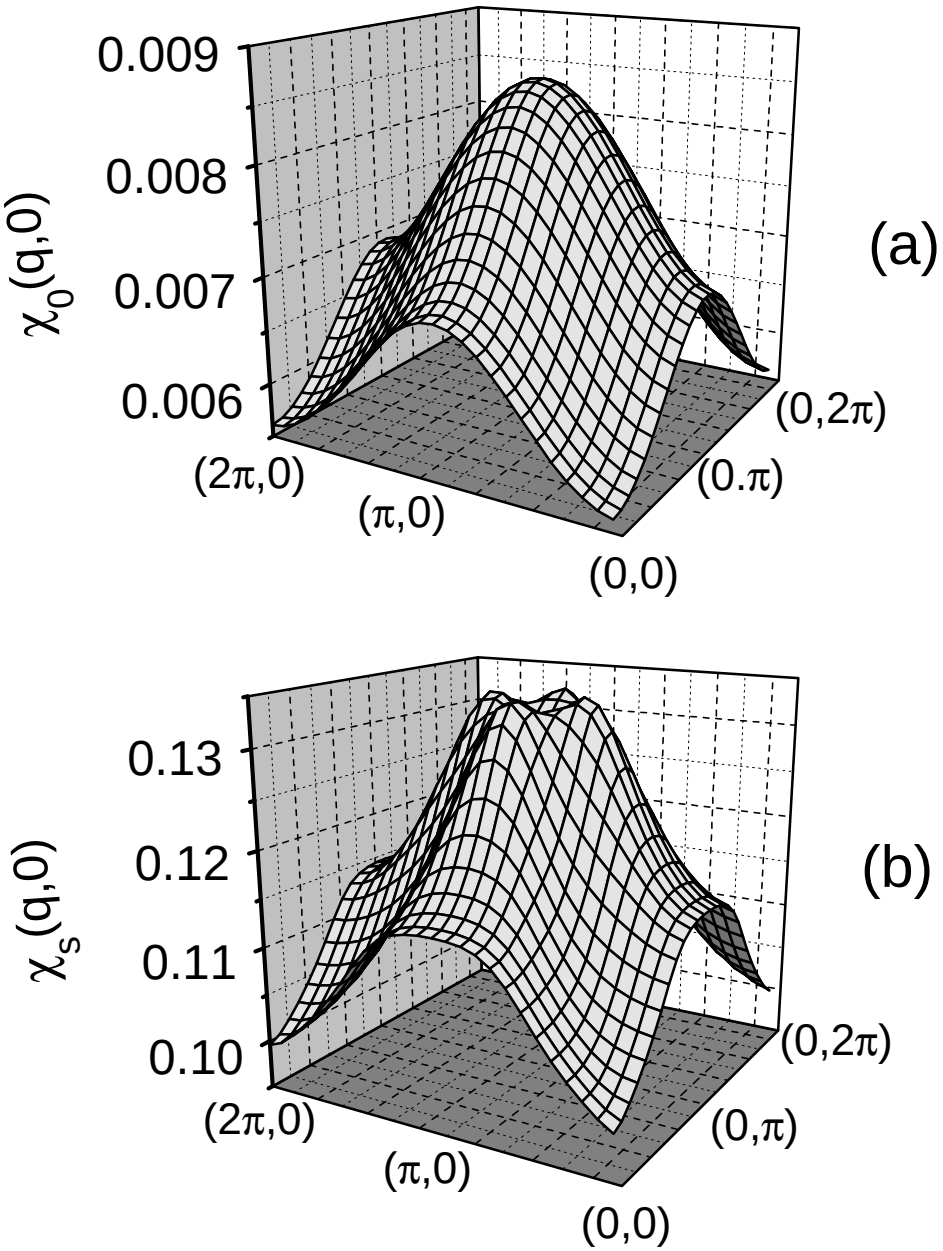
0.009
0.008
0.007
0.006
$\chi_0(q,0)$
(2π,0)
(π,0)
(0,0)
(0,2π)
(0.π)
(a)
0.13
0.12
0.11
0.10
$\chi_s(q,0)$
(2π,0)
(π,0)
(0,0)
(0,2π)
(0,π)
(b)